Design, synthesis, and biological assessment of a novel 1*H*-benzopyrazole derivative as an antimicrobial QSI and dual anticancer agent targeting A549 and MCF7 cell lines

Sunil Gadakh [1, 4], Rajendra S Mane* [1, 2], Tanay Ghoshal [3], Tushar Patel [4], Yadav Dilip [1], Suhas Janwadkar [1]

[1] *Department of Chemistry, S. D. Arts, V. S. A. Commerce & M. H. M. Science college, Palghar-401404, Maharashtra, India.*

[2] *Department of Chemistry, Dr. S. D. D. Arts College & Commerce & Science College, Wada-421303, Maharashtra, India.*

[3] *Department of Chemistry, Shri MM Patel Organization of Sciences, and research, Kadi university, Gandhinagar, Gujarat-382024, India.*

[4] *Piramal Discovery solution, Plot No 18, Pharmaceutical Special Economic Zone, Village Matoda, Ahmedabad, Gujarat 382213, India.*

Abstract: **Cancer and antimicrobial resistance (AMR) continue to pose significant threats to global health, necessitating the discovery of novel therapeutic agents with dual or multifunctional bioactivity. In this study, we report the rational design, synthesis, and biological evaluation of a novel benzopyrazole-tetrazole derivative (compound-6) targeting both cancer and quorum sensing (QS)-mediated microbial pathogenicity. The synthetic route involved a five-step sequence starting from 4-bromo-1*H*-indazole, incorporating key transformations such as *N*-alkylation, palladium-catalysed carboxylation, amide formation, nitrile conversion, and final tetrazole ring construction via [3+2] cycloaddition. The resulting compound-6 was evaluated for anticancer activity against A549 (lung) and MCF7 (breast) cancer cell lines, and for anti-QS activity using the 6CGY bacterial strain. Compound-6 exhibited excellent cytotoxicity, with IC_{50} values of 105.6 µM (A549) and 132.4 µM (MCF7), and demonstrated appreciable QS inhibition (anti-QS zone: 15.45 mm), albeit less potent than standard drugs Paclitaxel and Etoposide. These findings highlight the potential of benzopyrazole scaffolds as multifunctional bioactive agents, offering a promising platform for further structural optimization toward the development of dual-action anticancer and anti-virulence therapies.**

Keywords: **1H-Benzopyrazole derivatives, Antitumor activity, Lung cancer, Breast cancer, ADME study, Molecular Docking**

1. INTRODUCTION

Benzopyrazole is a significant aromatic heterocyclic compound featuring a fused ring system composed of a benzene ring and a pyrazole ring. Its chemical formula is $C_7H_6N_2$, and its unique structure makes it an essential compound in both organic chemistry and pharmaceutical sciences.

Key Characteristics of Benzopyrazole: Heterocyclic Structure: Benzopyrazole is a bicyclic system in which a benzene ring is fused with a five-membered pyrazole ring containing two nitrogen atoms. Aromaticity: The fused rings contribute to the compound's aromatic nature, enhancing its chemical stability. Chemical Reactivity: The nitrogen atoms in the pyrazole ring render the molecule chemically versatile, allowing it to undergo various substitution and functionalization reactions. Pharmaceutical Applications: Benzopyrazole derivatives have drawn considerable attention due to their diverse pharmacological activities, including anti-inflammatory, anticancer, antimicrobial, and antiviral properties. Additionally, they serve as precursors in the synthesis of advanced materials and dyes. Several clinically approved drugs and investigational agents are based on the benzopyrazole scaffold. Below are notable examples: Granisetron: A 5-HT3 receptor antagonist used to treat nausea and vomiting associated with chemotherapy and postoperative recovery. Niraparib (Zejula): An anticancer agent indicated for recurrent epithelial ovarian, fallopian tube, primary

peritoneal, breast, and prostate cancers. Pazopanib: A tyrosine kinase inhibitor approved for the treatment of renal cell carcinoma. Merestinib (LY2801653): An experimental cancer drug developed by Eli Lilly, functioning as a small molecule inhibitor targeting MET and several receptor tyrosine kinases (e.g., MST1R, FLT3, AXL, MERTK, TEK, ROS1, NTRK1/2/3, DDR1/2). CFI-400945: Investigated in clinical trials for advanced or metastatic breast cancer. Combination Therapy (Merestinib and LY2874455): Explored for its therapeutic potential in patients with relapsed or refractory acute myeloid leukemia [fig-1]

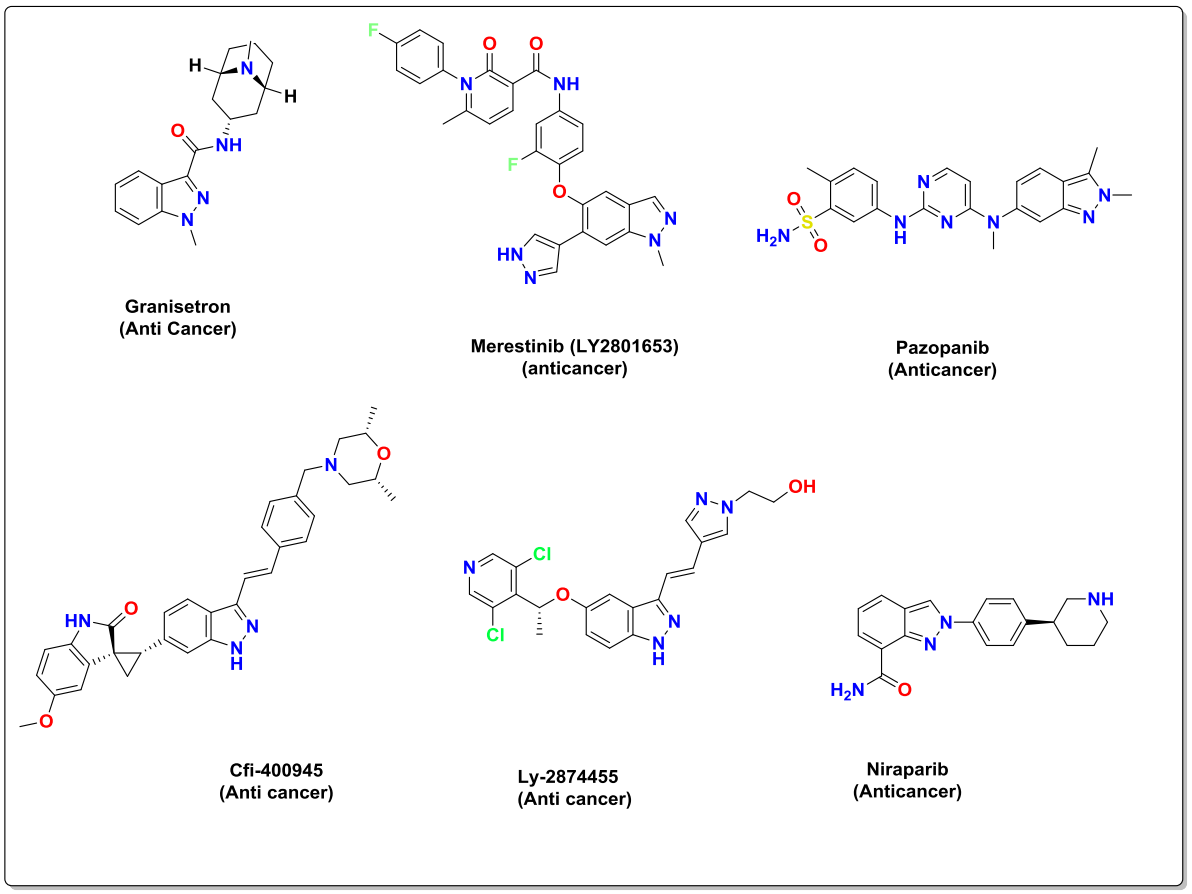

1. Benzopyrazole based marketed drugs

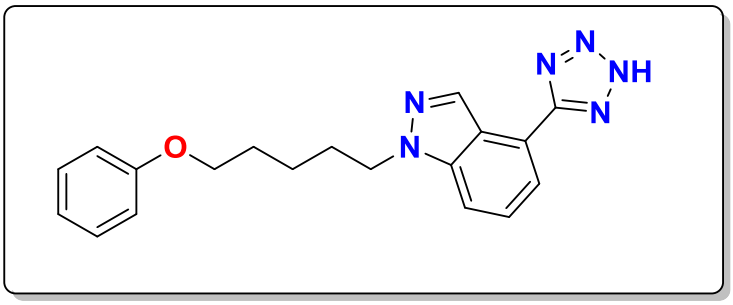

2. Designed Benzopyrazole Anti QSI and anticancer agents

Figure 1) Benzopyrazole based marketed drugs, 2) Designed Benzopyrazole antimicrobial and anticancer agents

Cancer remains one of the foremost challenges to global health, characterized by its high morbidity and mortality rates. Among the myriad forms of this disease, breast cancer and lung cancer are particularly prevalent, ranking as the most diagnosed and the leading causes of cancer-related deaths, respectively [1,2]. Despite advances in diagnosis, molecular profiling, and targeted therapies, treatment resistance, metastasis, and recurrence remain significant clinical hurdles. These challenges necessitate the continual development of novel chemotherapeutic agents with enhanced efficacy, selectivity, and safety profiles.

In this regard, heterocyclic compounds, particularly nitrogen-containing systems, have attracted

considerable attention in anticancer drug development due to their structural diversity and biological versatility [3]. One such privileged scaffold is benzopyrazole, a fused bicyclic heterocycle comprising a benzene ring fused to a pyrazole moiety. This unique structural framework endows benzopyrazoles with favourable pharmacokinetic properties and a broad spectrum of biological activities, including anti-inflammatory, antimicrobial, antioxidant, and notably, anticancer effects [4,5].

Recent studies have illuminated the therapeutic promise of benzopyrazole derivatives against various cancer types, with several molecules demonstrating significant cytotoxicity against breast (MCF-7, MDA-MB-231) and lung (A549, H1299) cancer cell lines [6–8]. The anticancer activity of benzopyrazole compounds is thought to be mediated through multiple mechanisms, such as the inhibition of topoisomerases, tyrosine kinases, tubulin polymerization, and the induction of apoptotic pathways [9]. Furthermore, structure–activity relationship (SAR) studies have revealed that substitutions on the pyrazole and benzene rings can dramatically influence biological potency and selectivity, offering a valuable platform for molecular optimization [10].

Moreover, benzopyrazole derivatives have demonstrated the ability to interfere with key signalling cascades such as PI3K/AKT/mTOR, MAPK/ERK, and EGFR/HER2, which are critically involved in tumour growth and survival [11,12]. In breast cancer, particularly triple-negative subtypes, and in non-small cell lung cancer (NSCLC), these pathways are often dysregulated, contributing to aggressive tumour behaviour and therapy resistance. Thus, the strategic design and synthesis of benzopyrazole-based small molecules offer a promising route to target these oncogenic pathways.

Given the considerations, the current study is aimed at the design, synthesis, and biological evaluation of novel benzopyrazole derivatives as potential antitumor agents against breast and lung cancer cell lines. By integrating rational drug design, synthetic chemistry, and in vitro biological screening, we endeavour to identify lead compounds with potent cytotoxic activity and favourable selectivity indices, paving the way for future preclinical investigations.

The global surge in antimicrobial resistance (AMR) has emerged as a critical public health crisis, largely driven by the overuse and misuse of conventional antibiotics. One of the pivotal bacterial survival strategies contributing to AMR is the quorum sensing (QS) system, a cell-density-dependent regulatory mechanism that controls gene expression related to virulence, motility, and biofilm formation in many pathogenic bacteria, including *Pseudomonas fluorescens*, *Salmonella enterica*, and *Staphylococcus epidermidis* [13]. Unlike traditional antibiotics that exert bactericidal or bacteriostatic effects, targeting QS offers a non-lethal strategy by attenuating pathogenic behaviour, thus reducing selective pressure for resistance development [14].

In this context, benzopyrazole derivatives, particularly those bearing heterocyclic modifications such as triazoles and pyrimidines, have garnered significant interest for their potential to disrupt QS-regulated pathways. Benzopyrazoles, which are fused heterocycles containing both a benzene and pyrazole ring, are known for a wide range of biological activities, including antibacterial, antifungal, and anti-inflammatory properties [15]. Recent studies have highlighted the promising role of benzopyrazole-based compounds as QS inhibitors (QSIs), capable of interfering with the *las*, *rhl*, and *pqs* systems in *Pseudomonas fluorescens* and other Gram-negative bacteria [16, 17].

For example, Mahmoud et al. synthesized a series of pyrazole and pyrazolo[1,5-a]pyrimidine derivatives that displayed potent antibiofilm and QS inhibitory activity. Compounds such as 3a and 10a showed over 80% inhibition of biofilm formation and significantly reduced pyocyanin production, swarming motility, and elastase activity in *Pseudomonas fluorescens* [4]. Similarly, triazole-linked 2-aminobenzimidazole hybrids developed by Kumar et al. demonstrated effective inhibition of the LasR-dependent QS system, with compound 6p showing potent anti-QS activity and favourable cytotoxicity profiles [17].

Given their structural flexibility and favourable pharmacokinetic properties, benzopyrazole derivatives offer a promising platform for the design of next-generation QSIs. Further exploration of their structure-activity relationships (SAR), along with in vivo efficacy and safety assessments, could pave the way for novel anti-virulence therapies that complement existing antimicrobial agents.

2. RESULTS AND DISCUSSION

2.1 Chemistry

The synthesis of 1*H*-benzopyrazole analogues was accomplished through a well-defined five-step

synthetic route, starting from 4-bromo-1*H*-indazole (CAS No. 186407-74-9) as the key intermediate. In the first step, selective *N*-alkylation at the *N*-1 position of 4-bromo-1*H*-indazole was achieved. This was carried out by deprotonating the indazole with sodium hydride (NaH) as a strong base in anhydrous tetrahydrofuran (THF) under inert atmosphere, followed by reaction with phenyl 5-bromopentyl ether (CAS No. 22921-72-8) at 70 °C. The reaction proceeded smoothly to furnish the intermediate 4-bromo-1-(5-phenoxypentyl)-1*H*-indazole 2 in good yield. This *N*-alkylation step is critical for introducing the 5-phenoxypentyl side chain, which plays an essential role in the final biological activity of the target analogues. In the second step, the aryl bromide moiety in compound 2 was transformed into a carboxylic acid via a palladium-catalysed carboxylation reaction. The reaction was conducted in dimethylformamide (DMF) as the solvent, using carbon dioxide (CO_2) as the C1 source. A suitable palladium catalyst, likely in the presence of a base such as a tertiary amine or carbonate, facilitated the oxidative addition and subsequent insertion of CO_2 into the aryl–Pd intermediate, yielding 1-(5-phenoxypentyl)-1*H*-indazole-4-carboxylic acid 3. The reaction afforded moderate yields, consistent with the challenges associated with direct carboxylation of aryl halides. The third step involved amide bond formation, where the carboxylic acid functionality of compound 3 was converted into the corresponding carboxamide. This was achieved using EDC·HCl (1-ethyl-3-(3-dimethylaminopropyl) carbodiimide hydrochloride) as the coupling reagent and HOBt (hydroxybenzotriazole) as the additive to suppress side reactions and improve coupling efficiency. The reaction was carried out in DMF, with ammonium chloride serving as the nitrogen source. The result was the successful formation of 1-(5-phenoxypentyl)-1*H*-indazole-4-carboxamide (compound 4), obtained in good yield. This amide linkage is a common motif in many bioactive heterocycles, enhancing both solubility and metabolic stability. In the fourth step, compound 4 underwent dehydration to yield the corresponding nitrile derivative. This transformation was accomplished using phosphorus oxychloride ($POCl_3$) as the dehydrating agent in toluene, a non-polar solvent that can withstand high temperatures. The reaction mixture was heated to 100 °C, leading to the conversion of the primary amide into the nitrile functional group, producing 1-(5-phenoxypentyl)-1*H*-indazole-4-carbonitrile (compound 5). This reaction likely proceeds through the formation of an imidoyl chloride intermediate, which is then eliminated to form the nitrile. The final step in the synthetic sequence involved the conversion of the nitrile group in compound 5 to a tetrazole ring, a key pharmacophoric group in various biologically active molecules. This was achieved through a [3+2] cycloaddition reaction between the nitrile group and sodium azide (NaN_3) in the presence of triethylamine hydrochloride, which likely serves to buffer the reaction and assist in solubilizing the azide. The reaction was conducted in DMF at 100 °C and stirred for 16 hours. This step yielded the final compound, 1-(5-phenoxypentyl)-1*H*-benzopyrazole tetrazole derivative (compound 6), completing the synthesis of the target molecule.

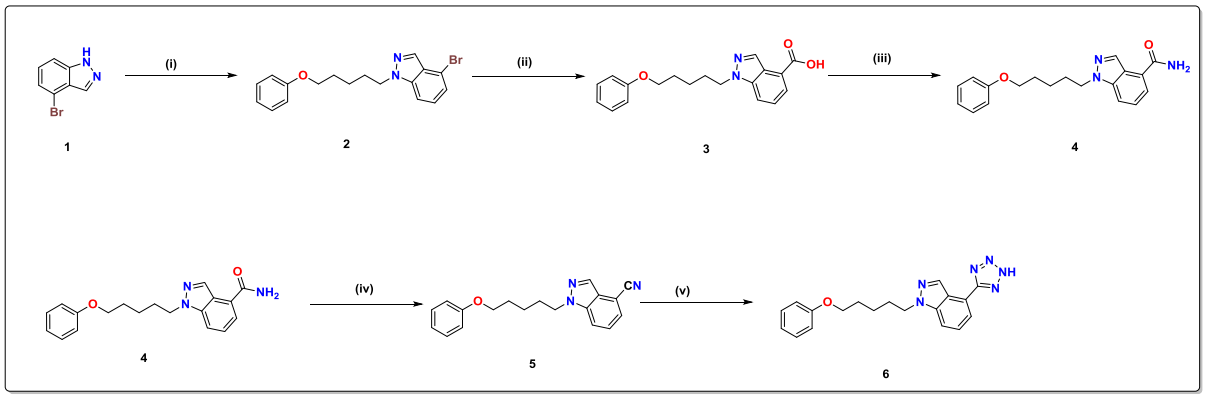

Scheme 1: Reagents and conditions: (i) NaH (1.50 eq), phenyl 5-bromopentyl ether (1.20 eq), THF, 70 °C, 2h. (ii) $PdCl_2$dppf.DCM complex (0.05eq), Xphos (0.1 eq), DMF, CO_2 (10 Kg/cm2), 100 °C, 16h (iii) EDC.HCl (1.5 eq), HOBt (1.5 eq), NH_4Cl (3.00 eq), DMF, rt, 2-3h, (iv) $POCl_3$, Toluene, 100 °C, (v) sodium azide (3.0eq), triethylamine hydrochloride (3.0 eq.), DMF, 100 °C, 16 h, 60-70%

3. MOLECULAR DOCKING

Molecular docking is a computational method for analysing receptor-ligand interactions, aiding drug discovery. In this study, docking was used to evaluate interactions between synthesized compounds and cancer-related proteins from lung (A549), breast (MCF7) and 6CGY cell line that protein structure corresponds to the *Pseudomonas fluorescens*. Chemical structures were drawn using ChemDraw Ultra 19.0, and docking studies were carried out with PyRx, utilizing AutoDock, AutoDock Vina, and Open Babel. Protein structures (PDB IDs corresponding to A549 and MCF7) were obtained from the RCSB Protein Data Bank and prepared in Discovery Studio 2024 by removing ligands, non-protein components, and water molecules, followed by the addition of polar hydrogens. Ligands and proteins were converted to pdbqt formats, and docking simulations were conducted to assess binding affinities and energy scores. The resulting protein-ligand complexes were visualized in 2D and 3D using Discovery Studio 2024 for further analysis.

3.1 Docking Results

3.1.1 Binding Affinities for A549 (Lung Cancer Cell Line)

Compound 6 demonstrated notable binding affinity towards the A549 lung cancer cell line, with a docking energy score of -3.8 kcal/mol. When compared to standard reference drugs, Paclitaxel and Etoposide, which exhibited docking energy scores of -3.0 kcal/mol and -7.0 kcal/mol respectively, compound 6 shows moderate affinity. Although not as strong as Etoposide, the result suggests potential inhibitory activity of compound 6 against lung cancer targets, warranting further investigation.

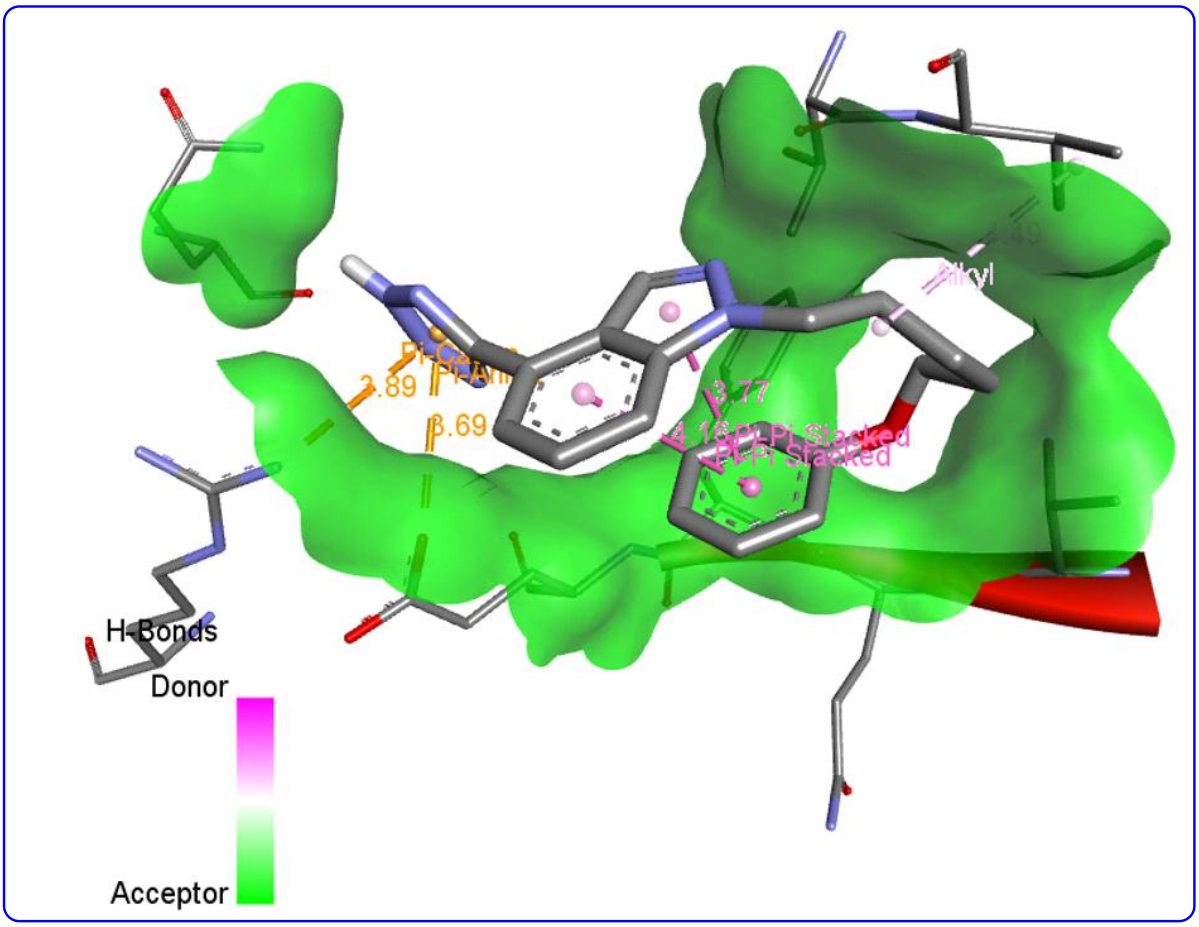

Fig-2: 3D interaction between Compound-6 and A549 Lung Cancer Cell Line

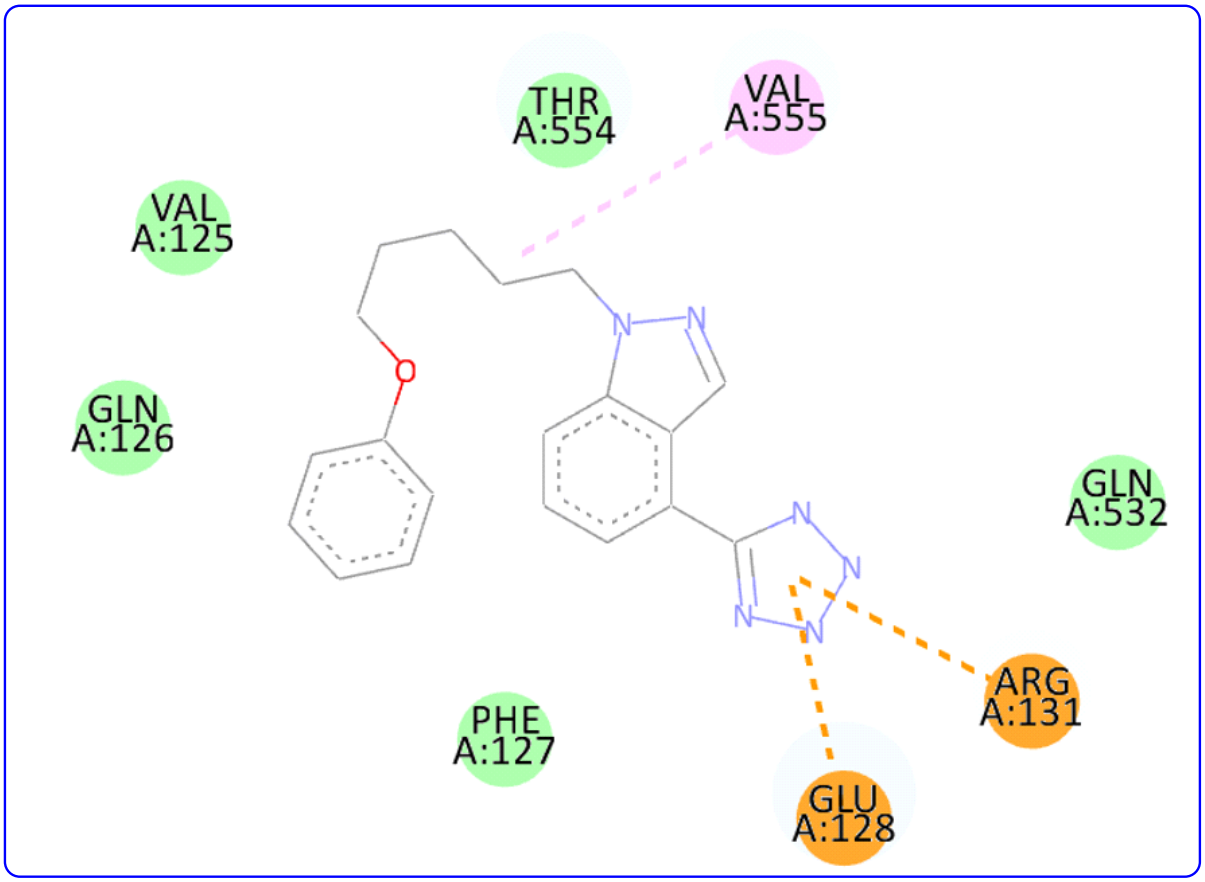

Fig-3: 2D interaction between Compound-6 and A549 Lung Cancer Cell Line

Multiple non-covalent interactions were observed between the ligand (UNK1) and nearby residues. A Pi-Cation interaction was noted between the positively charged NH2 group of ARG131 and the Pi-orbitals of UNK1 at 3.89 Å, indicating electrostatic stabilization. Similarly, a Pi-Anion interaction occurred between the negatively charged OE2 group of GLU128 and the Pi-orbitals of UNK1 at 3.69 Å. Two Pi-Pi stacked interactions were also detected between aromatic regions of the ligand itself, with distances of 4.16 Å and 3.77 Å, respectively, suggesting intramolecular stacking. Additionally, an Alkyl hydrophobic interaction was observed between VAL555 and UNK1 at 4.49 Å, further contributing to the overall ligand binding through non-polar contacts.

3.1.2 Binding Affinities for MCF-7 (Breast Cancer Cell Line)

In the case of the MCF-7 breast cancer cell line, compound 6 exhibited a significantly strong binding affinity, with a docking energy score of -7.7 kcal/mol. This value is comparable to, and even slightly more favorable than, the standard compounds Paclitaxel and Etoposide, which showed docking scores of -7.2 kcal/mol and -7.7 kcal/mol, respectively. The comparable performance of compound 6 to clinically used chemotherapeutic agents indicates its strong potential as a candidate for breast cancer treatment.

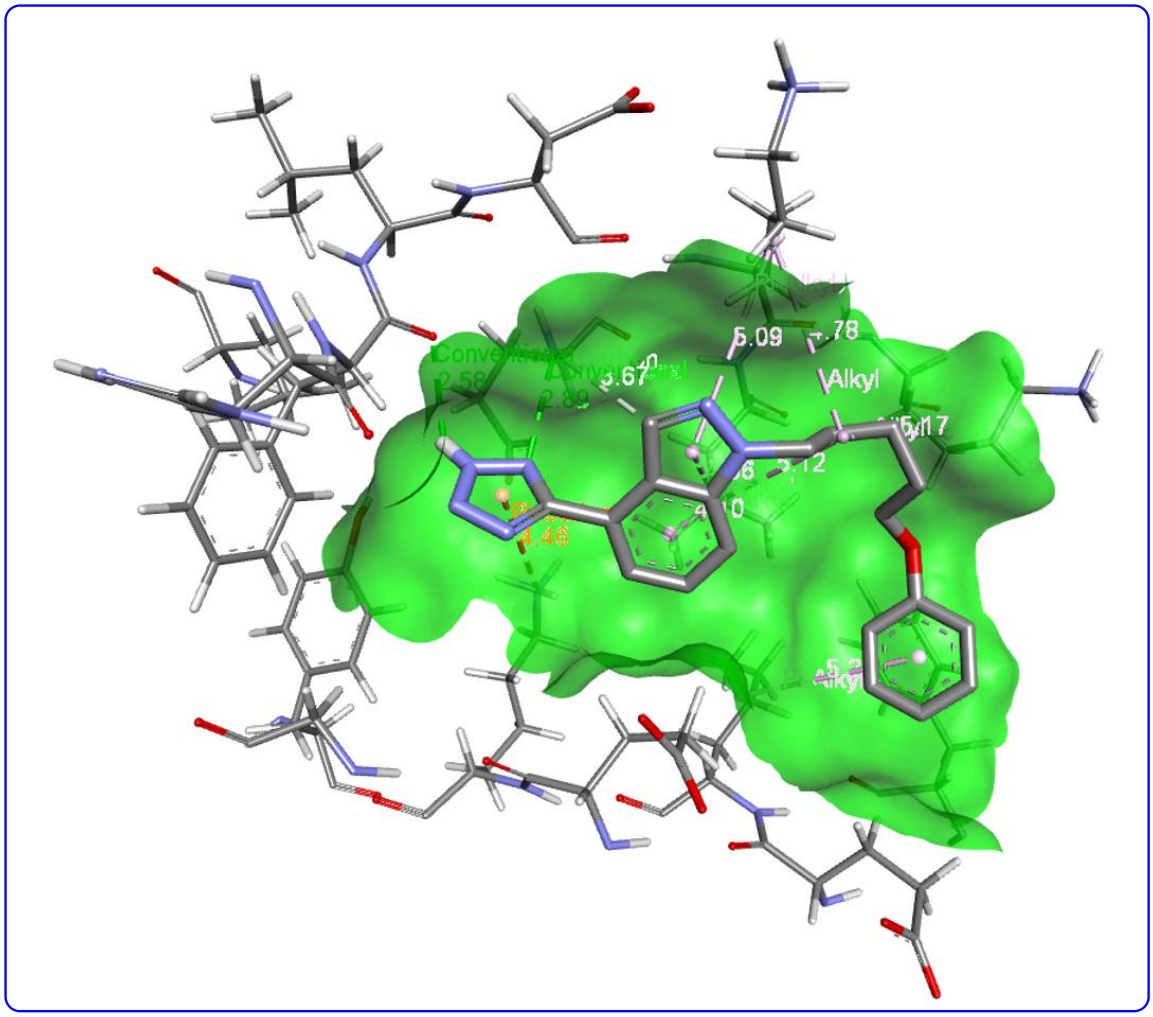

Fig-4: 3D Interaction between Compound-6 and MCF-7 Breast Cancer Cell Line

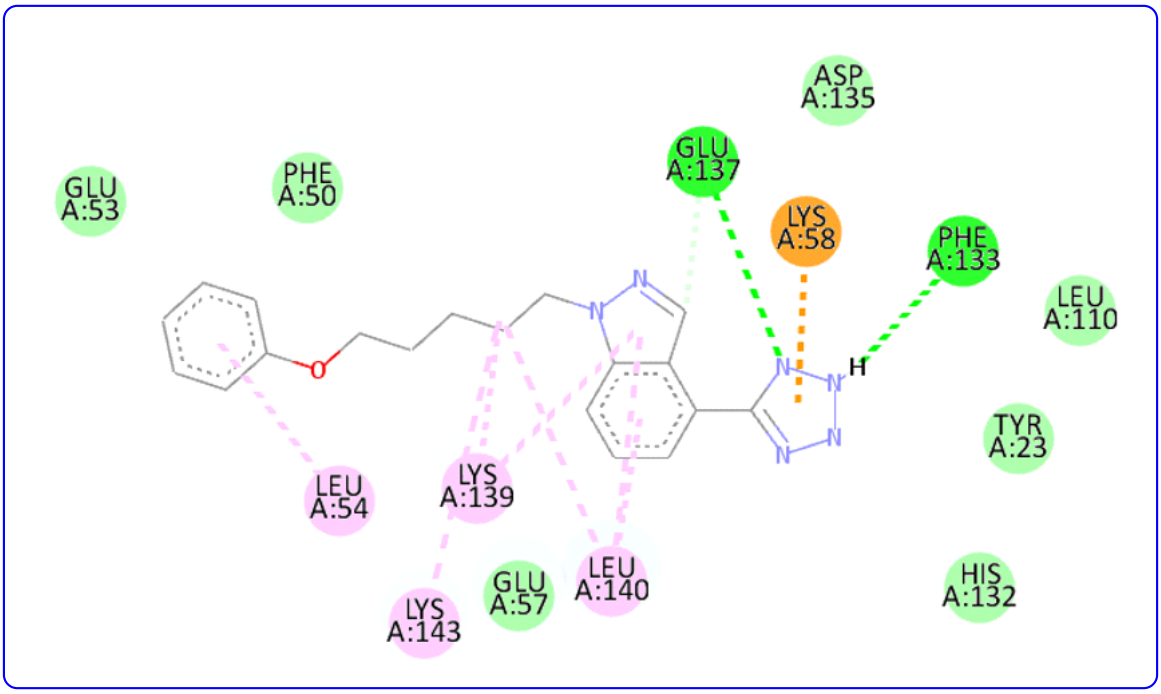

Fig-5: 2D interaction between Compound-6 and MCF-7 Breast Cancer Cell Line

A range of non-covalent interactions were identified between the ligand UNK1 and surrounding protein residues, highlighting its stable binding conformation. Notably, three hydrogen bonds were observed: two conventional hydrogen bonds were formed between the nitrogen of UNK1 and the nitrogen of GLU137 (2.89 Å), and between a hydrogen of UNK1 and the oxygen of PHE133 (2.58 Å). Additionally, a carbon-hydrogen bond was detected between the carbon of UNK1 and the nitrogen of GLU137 at 3.67 Å. A Pi-Cation electrostatic interaction was identified between the positively charged NZ group of LYS58 and the Pi-orbitals of UNK1 (4.46 Å). Multiple hydrophobic interactions further contribute to ligand stabilization, including alkyl interactions with LYS139 (4.78 Å), LYS143 (5.17 Å), and LEU140 (5.12 Å). Several Pi-Alkyl interactions were also observed between the Pi-orbitals of UNK1 and the alkyl side chains of LEU140 (4.10 Å and 4.86 Å), LYS139 (5.09 Å), and LEU54 (5.23 Å). Collectively, these hydrogen bonding, electrostatic, and hydrophobic contacts suggest a well-coordinated and favorable binding environment for the ligand.

3.1.3 Binding Affinities for 6CGY (Quorum Sensing Inhibitor Target)

Compound 6 also showed promising interaction with the 6CGY protein structure, a target associated with quorum sensing inhibition, with a docking energy score of -6.4 kcal/mol. In comparison, the standard compounds Paclitaxel and Etoposide both displayed stronger binding affinities, each with docking scores of -7.9 kcal/mol. While compound 6 is less potent than the reference drugs in this context, its affinity still suggests potential bioactivity in disrupting quorum sensing pathways, possibly contributing to anti-virulence or anti-bacterial properties.

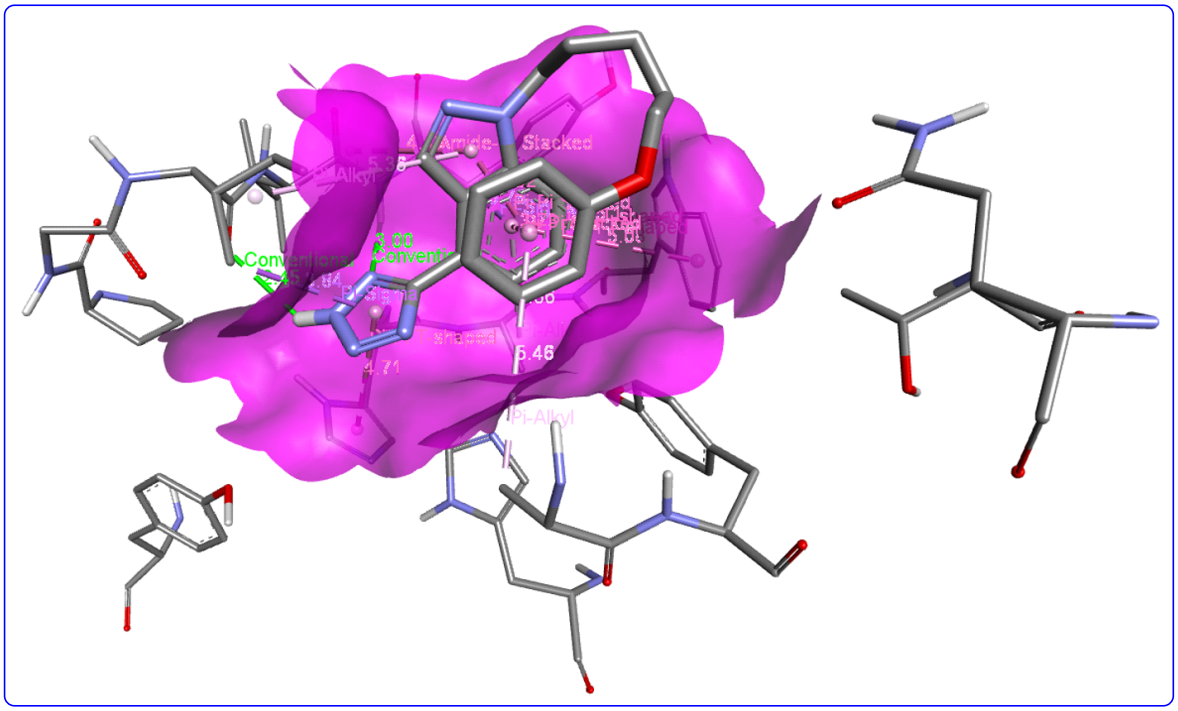

Fig-6: 3D Interaction between Compound-6 and 6CGY (Quorum Sensing Inhibitor Target)

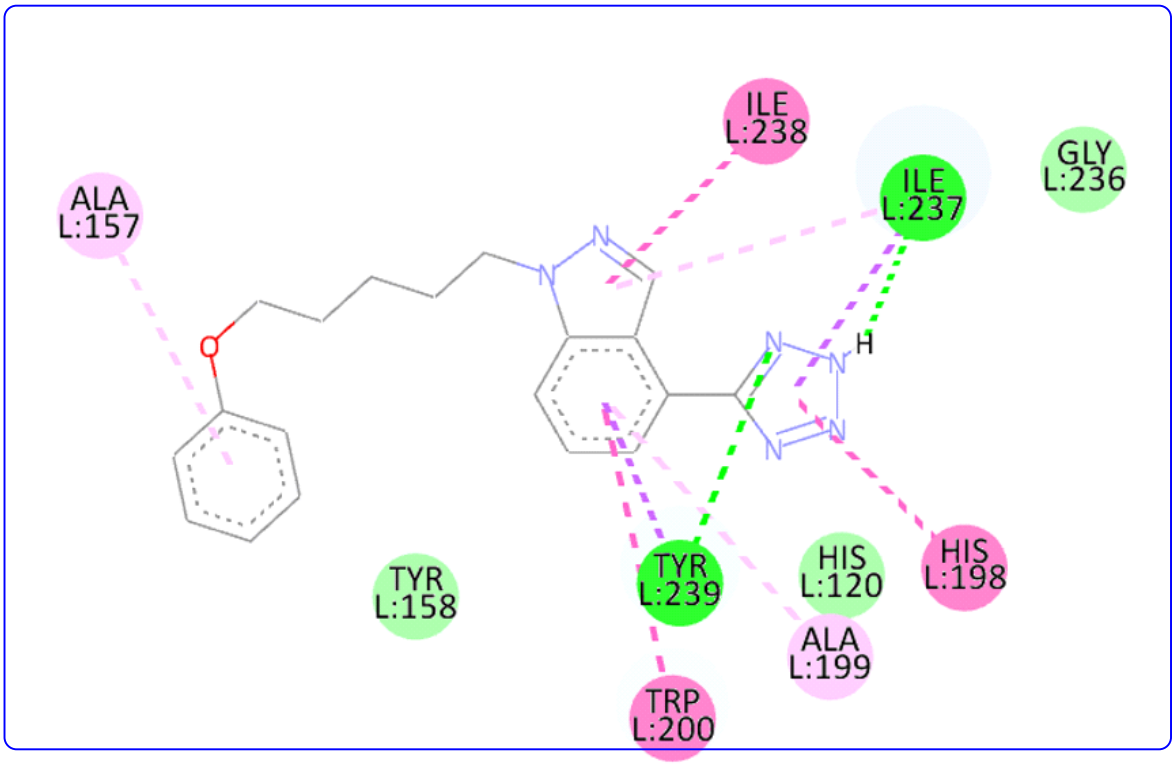

Fig-7: 2D Interaction between Compound-6 and 6CGY (Quorum Sensing Inhibitor Target)

Additional interactions between the ligand UNK1 and residues from the adjacent protein chain further contribute to its binding stability. Two conventional hydrogen bonds were observed: one between the HN group of TYR239 (as donor) and the nitrogen of UNK1 (as acceptor) at 3.00 Å, and another between a hydrogen of UNK1 and the oxygen of ILE237 at a distance of 2.45 Å. Hydrophobic Pi-Sigma interactions were also identified between the Pi-orbitals of UNK1 and the side chains of ILE237 (CG2) and TYR239 (CB), with bond distances of 3.84 Å and 3.79 Å, respectively. Two intramolecular Pi-Pi stacked interactions were again detected within UNK1 itself (3.73 Å and 3.92 Å), as well as three Pi-Pi T-shaped interactions involving aromatic residues HIS198 and TRP200 (ranging from 4.71 Å to 5.18 Å). An Amide-Pi stacking interaction was also observed between the amide group formed by ILE238:C, O and TYR239: N and the Pi-orbitals of UNK1 (4.40 Å). Furthermore, Pi-Alkyl interactions between the Pi-system of UNK1 and alkyl groups of ALA199 (5.36 Å), ILE237 (5.36 Å), and ALA157 (5.46 Å) contribute additional hydrophobic stabilization to the binding interface. These diverse interactions highlight a robust and multi-faceted binding mechanism between the ligand and its surrounding protein environment.

4. ADME STUDY

The synthesized molecules 6 were analysed using Molinspiration software to assess their ADME (Absorption, Distribution, Metabolism, and Excretion) profiles, compliance with Lipinski's Rule of Five, and key ADMET parameters. These evaluations were essential for determining the physicochemical and pharmacological properties of the compounds.

Molecule	Formula	MW	#Heavy atoms	#Aromatic heavy atoms	Fraction Csp3	#Rotatable bonds	#H-bond acceptors	#H-bond donors
6	C19H20N6O	348.4	26	20	0.26	8	5	1
	MR	TPSA	iLOGP	XLOGP3	WLOGP	MLOGP	Silicos-IT Log P	Consensus Log P
6	99.41	81.51	2.63	3.46	3.47	3.18	3.26	3.2
	ESOL Log S	ESOL Solubility	ESOL Solubility	ESOL Class	Ali Log S	Ali Solubility	Ali Solubility	Ali Class

		(mg/ml)	(mol/l)			(mg/ml)	(mol/l)	
6	-4.22	2.09E-02	6.01E-05	Moderately soluble	-4.85	4.88E-03	1.40E-05	Moderately soluble
	Silicos-IT LogSw	Silicos-IT Solubility (mg/ml)	Silicos-IT Solubility (mol/l)	Silicos-IT class	GI absorption	BBB permeant	Pgp substrate	CYP1A2 inhibitor
6	-6.94	4.01E-05	1.15E-07	Poorly soluble	High	No	No	Yes
	CYP2C19 inhibitor	CYP2C9 inhibitor	CYP2D6 inhibitor	CYP3A4 inhibitor	log Kp (cm/s)	Lipinski #violations	Ghose #violations	Veber #violations
6	Yes	Yes	No	Yes	-5.97	0	0	0
	Egan #violations	Muegge #violations	Bioavailability Score	PAINS #alerts	Brenk #alerts	Leadlikeness #violations	Synthetic Accessibility	
6	0	0	0.56	0	0	1	2.82	

Table-1: All ADME parameters for compound-6

Compound 6, with the molecular formula $C_{19}H_{20}N_6O$ and a molecular weight of 348.4 g/mol, consists of 26 heavy atoms, including 20 aromatic heavy atoms, and has a fraction of sp^3 carbons of 0.26. It possesses 8 rotatable bonds, 5 hydrogen bond acceptors, and 1 hydrogen bond donor, indicating moderate molecular flexibility and potential for intermolecular interactions. The compound's lipophilicity, evaluated using various models (iLOGP, XLOGP3, WLOGP, MLOGP, Silicos-IT), yields a consensus log P of 3.2, suggesting a balanced hydrophilic-lipophilic profile. The molecule's topological polar surface area (TPSA) is 81.51 $Å^2$, with a moderate molar refractivity of 99.41. In terms of solubility, molecule 6 is classified as moderately soluble according to both ESOL (log S = -4.22) and Ali models (log S = -4.85), while the Silicos-IT model categorizes it as poorly soluble (log S = -6.94). Despite this, it exhibits high gastrointestinal (GI) absorption and is not a substrate for P-glycoprotein (Pgp), which favors its oral bioavailability. The compound is predicted to inhibit several cytochrome P450 enzymes, including CYP1A2, CYP2C19, CYP2C9, and CYP3A4, but not CYP2D6, suggesting potential drug-drug interaction considerations. It is not blood-brain barrier (BBB) permeant and has a skin permeability log Kp of -5.97 cm/s, indicating limited dermal absorption. Crucially, molecule 6 complies fully with Lipinski's, Ghose's, Veber's, Egan's, and Muegge's rules, indicating good drug-likeness. It has a bioavailability score of 0.56 and shows no alerts for PAINS or Brenk structural filters, although it has one lead-likeness violation and a synthetic accessibility score of 2.82, suggesting it is relatively easy to synthesize. Overall, the molecule exhibits favourable ADME characteristics, making it a promising candidate for further pharmacological development

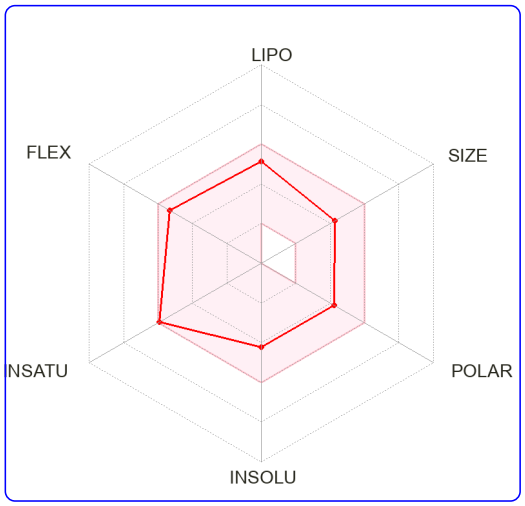

Fig-8: Toxicity contours for Synthesized compound-6

5. BIOLOGICAL ACTIVITY EVALUATION (METHODOLOGY) FOR A549 (LUNG CARCINOMA) AND MCF7 (BREAST ADENOCARCINOMA) CELL LINES

5.1 Cell Culturing and Maintenance: To assess the anticancer activity of the synthesized compounds, A549 (lung carcinoma) and MCF7 (breast adenocarcinoma) cell lines were procured from NCCS, Pune. Cells were cultured in DMEM with 10% inactivated FBS and 1% penicillin-streptomycin, and incubated at 37°C in 5% CO_2 until confluency. After discarding spent media and

washing with PBS, adherent cells were detached using 0.25% trypsin, centrifuged at 2000 rpm for 10 minutes, and the pellet was resuspended and subculture for further experiments.

5.2 Anticancer Activity (MTT Assay):

The anticancer activity was evaluated using the MTT assay. A549 and MCF7 cells were seeded at 7000 cells/well in 96-well plates and treated after 24 hours with test compounds (0.1–500 µM) dissolved in DMSO. Vehicle controls matched the DMSO concentration used in the 100 µM treatment. After 24 hours of treatment, cell viability was measured using the MTT assay per the manufacturer's protocol.

5.2.1 Calculation:

$$\left[\frac{A_1 - A_2}{A_1}\right] \times 100$$

A_1= Absorb of Untreated, A_2= Absorbance of Treated

6. BIOLOGICAL ACTIVITY EVALUATION FOR 6CGY (QUORUM SENSING INHIBITOR TARGET)

Bacterial Strains and Maintenance: *Pseudomonas fluorescens* PAO1 were kindly provided by Dr Sachin Sitapara, Department of Chemistry, Government Science college, Veraval, Gujarat 362265, INDIA. *Pseudomonas fluorescens* was cultured in King's B Medium (King's A or B), Mix culture with sterile 50% glycerol in a 1:1 ratio (final glycerol concentration = 25%), Aliquot into sterile cryovials and Store at -80°C and all Analytical-grade chemicals were used throughout this experiment

Extraction of Acyl-Homoserine Lactone (AHL): AHLs were extracted from *Pseudomonas fluorescens* PAO1 as per Pearson et al. (1995). Cultures were incubated at 37°C for 14–16 h, followed by extraction of the supernatant using acidified ethyl acetate. The organic phase was evaporated under reduced pressure to obtain purified AHL for quorum sensing assays.

7. RESULTS

The synthesized compound-6 was assessed for its anticancer and antimicrobial properties using three distinct cell lines: A549 (lung cancer), MCF7 (breast cancer), and 6CGY (quorum sensing inhibition). The biological evaluation aimed to compare the efficacy of compound-6 with that of well-established chemotherapeutic agents, Paclitaxel and Etoposide.

A549 Cell Line (Lung Cancer): Compound-6 demonstrated promising cytotoxic activity against the A549 cell line. The half-maximal inhibitory concentration (IC_{50}) was found to be 105.6 ± 10.21 µM, indicating a significant inhibitory effect. In comparison, the standard drugs Paclitaxel and Etoposide exhibited more potent cytotoxicity with IC_{50} values of 42.56 ± 1.34 µM and 58.31 ± 9.23 µM, respectively. Despite being less potent than the standards, compound-6 still showed noteworthy activity, suggesting its potential as a lead compound for further optimization.

MCF7 Cell Line (Breast Cancer): Against the MCF7 breast cancer cell line, compound-6 also exhibited notable cytotoxic activity with an IC_{50} value of 132.4 ± 22.48 µM. In contrast, Paclitaxel and Etoposide showed stronger inhibitory effects, with IC_{50} values of 43.18 ± 1.676 µM and 44.9 ± 8.12 µM, respectively. Although compound-6 was comparatively less potent, its moderate activity indicates a potential scaffold for the development of novel anticancer agents targeting breast cancer cells.

6CGY Cell Line (Quorum Sensing Inhibition - QSI): The antimicrobial potential of compound-6 was assessed using the 6CGY strain, with a focus on its quorum sensing inhibition (QSI) activity. The Anti-QS zone was measured to be 15.45 ± 5.43 mm, indicating substantial antimicrobial and anti-QS activity. Paclitaxel and Etoposide displayed larger inhibition zones of 25.82 ± 0.10 mm and 28.13 ± 0.45 mm, respectively. While the standard compounds exhibited stronger activity, compound-6 still demonstrated appreciable QSI capability, which may contribute to its overall antimicrobial profile.

Overall, compound-6 exhibited notable anticancer activity against both A549 and MCF7 cell lines and demonstrated significant anti-quorum sensing activity. Although its potency was lower than the standard chemotherapeutics, its consistent activity across all tested cell lines highlights its potential as a multifunctional bioactive molecule. Further structural optimization and mechanistic studies are warranted to enhance its efficacy and better understand its mode of action.

Sr. No.	Intermediate number	(A549 Cell Line) IC50 value	(MCF7 Cell Line) IC50 value	Anti-QS zone in mm *Pseudomonas fluorescens*

1	6	105.6±10.21	132.4±22.48	15.45 ± 5.43
2	Paclitaxel (Breast cancer)	42.56±1.34	43.18±1.676	25.82 ± 0.10
3	Etoposide (Lung's cancer)	58.31±9.23	44.9±8.12	28.13 ± 0.45

Table 2: IC_{50} values and Anti-QS zone in mm zone for compound 6 and standard compound Paclitaxel, Etoposide

8. STRUCTURE-ACTIVITY RELATIONSHIP (SAR):

The structure–activity relationship (SAR) analysis of ligand UNK1 reveals a robust and multifaceted binding mechanism driven by diverse non-covalent interactions. Key electrostatic contributions include Pi–Cation interactions with ARG131 (3.89 Å) and LYS58 (4.46 Å), and a Pi–Anion interaction with GLU128 (3.69 Å), enhancing ligand stabilization through charge–Pi orbital complementarity. A strong hydrogen bonding network further supports binding, with conventional hydrogen bonds involving GLU137, PHE133, TYR239, and ILE237 (ranging from 2.45 Å to 3.00 Å), along with a carbon–hydrogen bond with GLU137 (3.67 Å). Intramolecular Pi–Pi stacking interactions within UNK1 (3.73–4.16 Å) suggest a conformationally stable structure, while aromatic contacts with HIS198 and TRP200 via Pi–Pi T-shaped interactions (4.71–5.18 Å), and an Amide–Pi stacking with ILE238–TYR239 (4.40 Å) contribute to additional stabilization. Hydrophobic effects also play a major role, including alkyl and Pi–alkyl interactions with residues such as VAL555, LEU140, LYS139, and ALA199 (ranging from 4.10 Å to 5.46 Å), as well as Pi–Sigma interactions with ILE237 and TYR239. Collectively, these interactions provide a well-coordinated binding environment, indicating that the ligand's affinity is driven by a synergistic combination of electrostatics, hydrogen bonding, aromatic stacking, and hydrophobic contacts, making UNK1 a promising scaffold for further optimization.

Experimental Section

Melting Points: Determined using an Avi Scientific Blue Digital Melting Point Apparatus; values are uncorrected. NMR Spectroscopy: ^{1}H and ^{13}C NMR spectra were recorded on a Bruker Ascend™ 400 MHz spectrometer using TMS as the internal standard when applicable. Chemical shifts (δ, ppm) are reported relative to TMS. Splitting patterns: s (singlet), d (doublet), t (triplet), q (quartet), m (multiplet), br (broad). Solvents are noted in parentheses. Mass Analysis: ESI/mass spectra were acquired using a Shimadzu LC-MS QP1000 EX. Reagents and solvents were sourced from BLD Pharma (Hyderabad), Spectrochem (Pune), Combi-Blocks Ltd. (Delhi), and Merck (Mumbai). TLC Analysis: Conducted on Merck silica gel 60F-254 plates with mobile phases of hexane:ethyl acetate or DCM:methanol. Visualization used UV light or staining with $KMnO_4$, PMA, or ninhydrin. Purification: Performed via Combi-Flash chromatography with programmable injection; flow rates: 1–200 mL/min; pressure: up to 200 psi.

Synthesis of 4-bromo-1-[5-(phenoxy)pentyl]-1*H*-benzo[*d*]pyrazole [2]

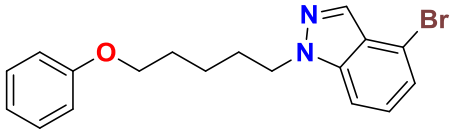

2

In a flame-dried, nitrogen-flushed 50 mL round-bottom flask equipped with a magnetic stir bar, 4-bromo-1*H*-benzo[*c*]pyrazole (10.0 g, 0.05076 mmol, 1.0 equivalents, CAS: 186407-74-9) was dissolved in anhydrous THF (100 mL) and cooled to 0 °C using an ice bath. To the stirred solution, sodium hydride (3.04 g, 60% dispersion in mineral oil, 0.07614 mmol, 1.5 equivalents) was added portion-wise over 15 minutes. The reaction mixture was stirred at 0 °C for an additional 30 minutes to ensure complete deprotonation. Phenyl 5-bromopentyl ether (14.8 g, 0.06091 mmol, 1.2 equivalents, CAS: 22921-72-8) was then added dropwise, and the reaction was warmed to 70 °C and stirred at that temperature for 2 hours under a nitrogen atmosphere. Reaction progress was monitored by

TLC. Upon completion, the reaction mixture was cooled to room temperature and quenched cautiously with ice-cold water (100 mL). The resulting mixture was extracted with ethyl acetate (3 × 250 mL). The combined organic layers were washed with brine, dried over anhydrous sodium sulphate, filtered, and concentrated under reduced pressure. The crude product was purified by column chromatography on silica gel using a hexane/ethyl acetate (9:1) gradient to yield 4-bromo-1-[5-(phenoxy) pentyl]-1*H*-benzo[*d*]pyrazole [2] as a white solid (17.5 g, 95% yield). ^{1}H NMR (400 MHz, DMSO): δ 1.25-1.31 (p, -CH_2-CH_2-CH_2-, 2H), 1.51-1.58 (p, -*N*-CH_2-CH_2-CH_2-, *J*=28MHz, 2H), 1.81-1.88 (p, O-CH_2-CH_2-CH_2-, *J*=28MHz, 2H), 3.36-3.40 (t, -*N*-CH_2-CH_2-, J=16MHz, 2H), 4.42-4.45 (t, O-CH_2-CH_2, J=12MHz, 2H), 7.24-7.38 (m, Ar-H+ Ph, J=32MHz, 7H), 7.74-7.76 (d, Ar-H, J=8MHz, 1H), 8.04 (s, Ar-H, 1H). ^{13}C NMR (400 MHz, DMSO-d6): 23.40 (H2C-C-CH_2), 29.24 (O-CH_2-C), 29.60 (*N*-CH2-C), 48.90 (-*N*-C-), 69.60 (-O-CH_2-Aliphatic), 109.99 (Ar-C), 113.63 (Ar-C-Br), 123.46 (Ar-C), 124.45 (Ar-C), 127.61 (Ar-C), 127.69 (Ar-C), 127.71 (Ar-C), 128.55 (Ar-C), 132.45 (Ar-C-CH_2-O), 139.09 (-*N*=C-), 140.12 (=*N*-C-). ESI-MS m/z of 359.12, 361.13, Bromo pattern, [M, M+2] $^{+}$. (TLC System Hexane: Ethyl acetate 8:2, Rf=0.57cm).

Synthesis of 1-(5-phenoxypentyl)-1*H*-benzo[*d*]pyrazole-4-carboxylic acid [3]

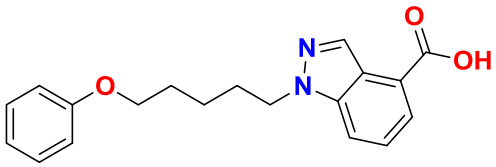

3

To a solution of 4-bromo-1-[5-(phenoxy) pentyl]-1H-benzo[d]pyrazole [2] (17.0 g, 0.0473 mol, 1.0 equivalents) in dry N, N-dimethylformamide (DMF), palladium (II) chloride complex with 1,1′-bis(diphenylphosphino)ferrocene ($PdCl_2$(dppf), 3.4 g, 0.00473 mol, 0.1 equivalents) and XPhos (4.5 g, 0.00946 mol, 0.2 equivalents) were added under a nitrogen atmosphere. The reaction vessel was sealed and charged with carbon dioxide gas to a pressure of 10 kg/cm². The mixture was then heated to 100 °C and stirred for 16 hours under these conditions, with pressure closely monitored throughout the reaction. Upon completion, the vessel was removed from heat and allowed to cool to room temperature. The CO_2 gas was carefully released by slow depressurization. The reaction solvent was removed under reduced pressure using a rotary evaporator. The resulting residue was extracted with ethyl acetate, and the organic layer was washed sequentially with water and brine to remove water-soluble impurities. The organic phase was dried over anhydrous sodium sulfate (Na_2SO_4), filtered, and concentrated under reduced pressure to yield the crude product. Purification was carried out by column chromatography on silica gel using a 0–10% gradient of methanol in dichloromethane (DCM) as the eluent. The appropriate fractions were collected and concentrated under vacuum to afford the desired product, 1-(5-phenoxypentyl)-1*H*-benzo[*d*]pyrazole-4-carboxylic acid [3], as a white solid (13.8 g, 89.9% yield). Spectral Data: ^{1}H NMR (400 MHz, DMSO-d_6) δ: 1.30–1.32 (p, CH_2–CH_2–CH_2, J = 8 Hz, 2H), 1.56–1.59 (p, N–CH_2–CH_2–CH_2, J = 12 Hz, 2H), 1.93–1.96 (p, O–CH_2–CH_2–CH_2, J = 12 Hz, 2H), 3.36–3.39 (t, N–CH_2–CH_2, J = 12 Hz, 2H), 4.49–4.52 (t, O–CH_2–CH_2, J = 12 Hz, 2H), 7.27–7.38 (m, Ar–H + Ph, J = 32 Hz, 6H), 7.78–7.80 (d, Ar–H, J = 8 Hz, 1H), 7.90–7.92 (d, Ar–H, J = 8 Hz, 1H), 8.64 (s, Ar–H, 1H), 12.97 (br s, –COOH, 1H). ^{13}C NMR (400 MHz, DMSO-d_6) δ: 23.21 (CH_2–CH_2–CH_2), 29.10 (N–CH_2–CH_2), 30.27 (O–CH_2–CH_2), 53.19 (N–CH_2), 69.70 (O–CH_2), 119.89, 123.12, 123.59, 125.20, 125.40, 125.45, 127.60, 127.71, 128.56 (aromatic C), 139.01 (N=C), 148.75 (Ar–C–N), 167.52 (COOH). ESI-MS: m/z = 325.45 $[M + H]^+$. TLC: R_f = 0.23 (ethyl acetate, 100%).

Synthesis of 1-(5-phenoxypentyl)-1*H*-benzopyrazole-4-carboxamide [4]

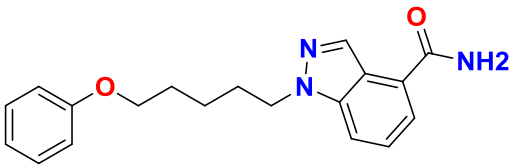

4

To a dry round-bottom flask equipped with a magnetic stir bar, 1-(5-phenoxypentyl)-1*H*-benzo[*d*]pyrazole-4-carboxylic acid [3] (13.0 g, 0.0410 mol, 1.0 equivalents) was dissolved in anhydrous N,N-dimethylformamide (DMF, 130 mL) under ambient conditions. To this solution, 1-hydroxybenzotriazole (HOBt, 8.1 g, 0.0601 mol, 1.5 equivalents) was added, and the mixture was stirred for a few minutes until fully dissolved. Subsequently, N-(3-dimethylaminopropyl)-N′-ethylcarbodiimide hydrochloride (EDC·HCl, 11.4 g, 0.0601 mol, 1.5 equivalents) was added, and the reaction mixture was stirred for an additional 10 minutes to allow activation of the carboxylic acid.

Ammonium chloride (NH_4Cl, 10.8 g, 0.205 mol, 5.0 equivalents) was then added directly to the mixture, which was stirred at room temperature for 3 hours. Reaction progress was monitored by thin-layer chromatography (TLC). Upon completion, the reaction was quenched with cold water, and the resulting aqueous phase was extracted with ethyl acetate. The combined organic extracts were washed with brine, dried over anhydrous sodium sulfate (Na_2SO_4), filtered, and concentrated under reduced pressure. The crude product was purified by column chromatography on silica gel using a gradient of hexane and ethyl acetate (0–100%) as eluent to afford the desired amide product, 1-(5-phenoxypentyl)-1*H*-benzo[*d*]pyrazole-4-carboxamide [4], as a solid (11.0 g, 84% yield). Spectral Data: ^{1}H NMR (400 MHz, DMSO-d_6) δ: 1.24–1.32 (p, CH_2–CH_2–CH_2, J = 32 Hz, 2H), 1.52–1.59 (p, N–CH_2–CH_2–CH_2, 2H), 1.88–1.96 (p, O–CH_2–CH_2–CH_2, J = 40 Hz, 2H), 3.36–3.39 (t, N–CH_2, J = 12 Hz, 2H), 4.44–4.47 (t, O–CH_2, J = 12 Hz, 2H), 7.24–7.32 (m, Ar–H, J = 32 Hz, 6H), 7.36 (br s, –$CONH_2$, 1H), 7.59–7.61 (d, Ar–H, J = 8 Hz, 1H), 7.76–7.78 (d, Ar–H, J = 8 Hz, 1H), 7.95 (br s, –$CONH_2$, 1H), 8.65 (s, Ar–H, 1H). ^{13}C NMR (400 MHz, DMSO-d_6) δ: 23.30 (CH_2–CH_2–CH_2), 29.15 (N–CH_2–CH_2–CH_2), 30.23 (O–CH_2–CH_2–CH_2), 53.26 (N–CH_2), 69.20 (O–CH_2), 119.23, 121.92, 121.64, 124.75, 125.53, 125.41, 126.61, 127.50 (aromatic C), 139.01 (N=C), 148.09 (Ar–C–N), 168.55 ($CONH_2$).ESI-MS: m/z = 324.40 $[M + H]^+$. TLC: R_f = 0.26 (ethyl acetate).

Step-26: Synthesis of 1-(5-Phenoxypentyl)-1*H*-benzo[*d*]pyrazole-4-carbonitrile [5]

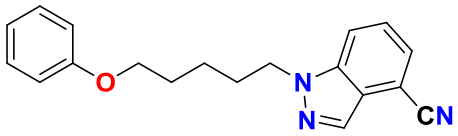

5

To a dry 250 mL round-bottom flask equipped with a magnetic stir bar and fitted with a reflux condenser, 1-(5-phenoxypentyl)-1*H*-benzo[*d*]pyrazole-4-carboxamide [4] (10.0 g, 30.96 mmol, 1.0 equivalents) was added, followed by phosphorus oxychloride ($POCl_3$, 30 mL, 93 mmol, 3.0 equivalents). The mixture was stirred at room temperature for 10–15 minutes to ensure homogeneity, then heated to reflux (~105 °C) under a nitrogen atmosphere. The reaction was stirred at reflux for 5 hours while monitoring the progress by thin-layer chromatography (TLC). After completion, the reaction mixture was cooled to room temperature and cautiously poured onto crushed ice with vigorous stirring, ensuring controlled addition to manage the exothermic reaction. The aqueous phase was carefully neutralized with saturated sodium bicarbonate solution until gas evolution ceased and pH approached neutral. The resulting mixture was extracted with ethyl acetate (3 × 50 mL). The combined organic layers were washed with brine (1 × 50 mL), dried over anhydrous sodium sulfate (Na_2SO_4), filtered, and concentrated under reduced pressure. The crude product was purified by column chromatography on silica gel using a gradient of hexane/ethyl acetate (70:30) as the eluent, affording 1-(5-Phenoxypentyl)-1*H*-benzo[*d*]pyrazole-4-carbonitrile [5] as a solid. (8.3 g, 87% yield).

Caution: $POCl_3$ is highly corrosive and toxic. All operations should be carried out in a well-ventilated fume hood with appropriate PPE, and neutralization should be performed slowly to prevent excessive bubbling and splashing. ^{1}H NMR (400 MHz, DMSO-d6): δ 1.23-1.31 (p, CH2-CH2-CH2-, J=32MHz, 2H), 1.51-1.58 (p, N-CH2-CH2-CH2-, J=28MHz, 2H), 1.82-1.89 (p, O-CH2-CH2-CH2-, J=28MHz, 2H), 3.36-3.40 (t, -N-CH2-CH2-, J=16MHz, 2H), 4.49-4.53 (t, O-CH2-CH2, J=16MHz, 2H), 7.23-7.34 (m, Ar-H +Ph, J=44MHz, 5H), 7.54-7.58 (t, Ar-H, J=16MHz, 1H), 7.74-7.76 (d, Ar-H, J=8MHz, 1H), 8.13-8.15 (d, Ar-H, J=8MHz, 1H), 8.30 (s, Ar-H, 1H). ^{13}C NMR (400 MHz, DMSO-d6): 23.21 (H2C-CH2-CH2), 29.07 (N-CH2-CH2-), 29.52 (-O-CH2-CH2-), 48.60 (-N-CH2-), 69.56 (-O-CH2-), 102.51 (Ar-C-Cyano), 116.09 (Ar-C), 117.69 (-CN-), 123.11 (Ar-C), 126.23 (Ar-C), 127.40 (Ar-C), 127.69 (Ar-C), 127.52 (Ar-C), 128.57 (Ar-C), 131.11 (-N=C-), 139.11 (Ph-C-CH2-O), 139.30 (-N-C=). ESI-MS m/z of 306.22 $[M+1]^+$. (TLC System Hexane: Ethyl acetate 7:3, Rf= 0.51cm).

Synthesis of 1-(5-Phenoxypentyl)-4-(1*H*-tetrazol-5-yl)-1*H*-benzo[*d*]pyrazole [6]

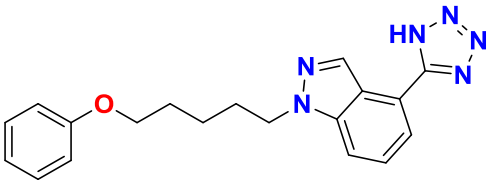

6

To a solution of 1-(5-Phenoxypentyl)-1*H*-benzo[*d*]pyrazole-4-carbonitrile [5] (5.00 g, 1.00 equivalents, 0.01639 mmol) in dry DMF (50 mL), triethylamine hydrochloride (11.2 g, 5.00

equivalents, 0.08196 mmol) and sodium azide (NaN_3, 4.4 g, 5.00 equivalents, 0.08196 mmol) were added under a nitrogen atmosphere at room temperature. The reaction mixture was heated to 100°C and stirred for 16 hours. After completion, the reaction mass was allowed to cool to room temperature, and cold water was added. The reaction mixture was then extracted with ethyl acetate. The combined ethyl acetate extracts were washed with water and brine, and the organic layer was dried over anhydrous sodium sulfate. The solution was filtered and concentrated under reduced pressure to give the crude product. The crude product was purified by column chromatography using 60-120 mesh silica gel and a gradient of 0-5% methanol in dichloromethane (DCM) as the eluent, yielding 1-(5-Phenoxypentyl)-4-(1H-tetrazol-5-yl)-1H-benzo[d]pyrazole [6] (5.0 g, 87% yield). Spectral Data: ^{1}H NMR (400 MHz, DMSO-d_6) δ: 1.29 (br s, CH_2–CH_2–CH_2–, 2H), 1.56 (br s, N–CH_2–CH_2–CH_2–, 2H), 2.09 (br s, O–CH_2–CH_2–CH_2–, 2H), 3.28 (br s, O–N–CH_2–, 2H), 4.39 (br s, O–CH_2–, 2H), 7.25–7.29 (m, Ar-H + Ph, J = 16 Hz, 5H), 7.60 (m, Ar-H, 1H), 7.95 (m, Ar-H, 1H), 7.97 (m, Ar-H, 1H), 8.62 (s, Ar-H, 1H). ^{13}C NMR (400 MHz, DMSO-d_6) δ: 23.12 (CH_2–CH_2–CH_2–), 29.04 (*N*–CH_2–CH_2–), 29.61 (O–CH_2–CH_2–), 48.60 (*N*–CH_2–), 69.71 (O–CH_2–), 113.24 (Ar-C), 117.03 (Ar-C), 120.41 (Ar-C), 120.53 (Ar-C–Tetrazole), 126.41 (Ar-C), 127.73 (Ar-C), 127.85 (Ar-C), 128.22 (Ar-C), 133.17 (Ar-C–CH_2–O), 139.22 (–C≡N), 140.12 (=C–*N*). ESI-MS: m/z = 349 $[M + H]^+$, TLC: DCM: MeOH, 9:1, Rf = 0.12 cm.

ACKNOWLEDGEMENTS

The authors express their sincere gratitude to Piramal Pharma Ltd., Plot No. 18, Pharmaceutical SEZ, Village Matoda, Ahmedabad, Gujarat-382213, and the Principal and Department of Chemistry, Sonopant Dandekar College, Palghar, Kharekuran Road, District: Thane, Maharashtra 401404, for their invaluable support for this research study. Special thanks to Dr. Sachin M. Sitapara, Assistant Professor of Chemistry, Government Science College, Veraval, Gujarat-362265, India, for his assistance and support in conducting the research.

REFERENCES

[1] Sung H, et al. Global cancer statistics 2020: *GLOBOCAN estimates of incidence and mortality worldwide for 36 cancers in 185 countries.* CA Cancer J Clin. 2021;71(3):209–249. *https://doi.org/10.3322/caac.21660*

[2] Siegel RL, et al. *Cancer statistics, 2024.* CA Cancer J Clin. 2024;74(1):12–44. *https://doi.org/10.3322/caac.21785*

[3] Khan I, et al. Heterocyclic compounds: A rich source of pharmacologically active *molecules.* Future Med Chem. 2020;12(2):147–190. *https://doi.org/10.4155/fmc-2019-0162*

[4] Patel NB, et al. Benzopyrazole derivatives: Synthesis, biological evaluation, and anticancer potential. *Eur J Med Chem*. 2021; 209:112862. *https://doi.org/10.1016/j.ejmech.2020.112862*

[5] Gaba M, et al. Pyrazole-based medicinal chemistry: A review. *Eur J Med Chem*. 2019; 164:201–240. *https://doi.org/10.1016/j.ejmech.2018.12.036*

[6] Rani N, et al. Design and synthesis of novel benzopyrazoles as anticancer agents: In vitro cytotoxicity and molecular docking studies. *Bioorg Med Chem Lett*. 2020;30(16):127310. *https://doi.org/10.1016/j.bmcl.2020.127310*

[7] Ahmad A, et al. Targeting breast cancer stem cells with novel benzopyrazole analogs: Insights from biological and in silico studies. *Sci Rep*. 2022; 12:4567. *https://doi.org/10.1038/s41598-022-08594-z*

[8] Kaur H, et al. Benzopyrazole analogues as potential inhibitors of EGFR in lung cancer models. *Bioorg Chem*. 2023; 138:106576. *https://doi.org/10.1016/j.bioorg.2023.106576*

[9] Yu Y, et al. Mechanistic insight into the anticancer activity of pyrazole-based hybrids: Tubulin inhibition and cell cycle arrest. *Eur J Med Chem*. 2021; 213:113180. *https://doi.org/10.1016/j.ejmech.2021.113180*

[10] Bansal Y, Silakari O. Structure-activity relationship studies on benzopyrazoles as kinase inhibitors: Recent advances and future prospects. *Curr Med Chem.* 2020;27(30):5005–5032. *https://doi.org/10.2174/0929867326666190912114720*

[11] Liu Z, et al. Targeting PI3K/AKT/mTOR signaling in cancer with pyrazole-based compounds. *Eur J Med Chem*. 2022; 230:114118. *https://doi.org/10.1016/j.ejmech.2022.114118*

[12] Verma A, et al. Novel benzopyrazole scaffolds modulate MAPK/ERK and EGFR signaling in cancer cells. *Med Chem Res.* 2023; 32:1163–1174. *https://doi.org/10.1007/s00044-023-03070-5*

[13] LaSarre, B., & Federle, M. J. (2013). Exploiting Quorum Sensing to Confuse Bacterial Pathogens. *Microbiology and Molecular Biology Reviews*, 77(1), 73–111. *https://doi.org/10.1128/MMBR.00046-12*

[14] Defoirdt, T., Boon, N., Bossier, P., & Verstraete, W. (2004). Disruption of bacterial quorum sensing: an unexplored strategy to fight infections in aquaculture. *Aquaculture*, 240(1-4), 69–88. *https://doi.org/10.1016/j.aquaculture.2004.06.031*

[15] Jafari, E., & Khajouei, M. R. (2020). Pyrazole and its derivatives: A review of their structures, synthesis, and biological activities. *Chemistry & Biodiversity*, 17(5), e1900582. *https://doi.org/10.1002/cbdv.201900582*

[16] Mahmoud, A. M., Emran, M. Y., Ghaly, M. A., et al. (2023). Design, synthesis and biological evaluation of pyrazole and pyrazolo[1,5-a] pyrimidine derivatives as antimicrobial agents targeting quorum sensing and biofilm formation. *Antibiotics*, 12(1), 128. *https://doi.org/10.3390/antibiotics12010128*

[17] Kumar, R., Kaur, G., Rajput, S., et al. (2022). Triazole-linked 2-aminobenzimidazoles as LasR inhibitors for the treatment of *Pseudomonas fluorescens* infections. *Bioorganic Chemistry*, 124, 105805. *https://doi.org/10.1016/j.bioorg.2022.105805*